Duplexed Imaging

International Edition: DOI: 10.1002/anie.201601233
German Edition: DOI: 10.1002/ange.201601233

A Single Excitation-Duplexed Imaging Strategy for Profiling Cell Surface Protein-Specific Glycoforms

Na Wu, Lei Bao, Lin Ding, and Huangxian Ju**

Abstract: *This work develops a site-specific duplexed luminescence resonance energy transfer system on cell surface for simultaneous imaging of two kinds of monosaccharides on a specific protein by single near-infrared excitation. The single excitation-duplexed imaging system utilizes aptamer modified upconversion luminescent nanoparticles as an energy donor to target the protein, and two fluorescent dye acceptors to tag two kinds of cell surface monosaccharides by a dual metabolic labeling technique. Upon excitation at 980 nm, only the dyes linked to protein-specific glycans can be lit up by the donor by two parallel energy transfer processes, for in situ duplexed imaging of glycoforms on specific protein. Using MUC1 as the model, this strategy can visualize distinct glycoforms of MUC1 on various cell types and quantitatively track terminal monosaccharide pattern. This approach provides a versatile platform for profiling protein-specific glycoforms, thus contributing to the study of the regulation mechanisms of protein functions by glycosylation.*

In eukaryotic cells, most of cell surface proteins are covalently attached to sugar chains, a repertoire of extremely diverse structures composed of several monosaccharide building blocks.[1] The unique glycosylation pattern, a population of glycoforms that share the same polypeptide backbone,[2a] serves as an important determinant for protein conformation and activity,[1c,2] and in turn, these glycoforms are regulated by a particular set of signal pathways.[1] Moreover, the variation of the glycan structures of a certain glycoprotein can be closely linked with specific changes of cell physiological states.[1] Thus in situ visualization of glycoforms of a given glycoprotein on a cell surface can contribute to the understanding of glycosylation machinery and its pleiotropic regulation of biological functions, and the identification of new diagnostic biomarkers as well as therapeutic targets.[2b]

Fluorescence resonance energy transfer (FRET)-based imaging technique has offered an attractive solution for imaging monosaccharides on specific cell surface proteins, such as EGFR,[3a] integrin $\alpha_v\beta_3$,[3b] and $\alpha_X\beta_2$,[3c] as well as intracellular proteins.[3d,e] These strategies rely on the respective labeling of protein and monosaccharide with donor and acceptor, and the emergence of FRET,[3] thus allowing the detection of only one kind of monosaccharide. Considering the diversity and complexity of the glycoforms,[1,2] profiling multiple monosaccharides on a given cell surface protein is very significant for revealing complex glycan-regulated signal pathway machinery.[1] Virtually no progress has been made in this challenging field owing to the difficulty in obtaining appropriate pairs of donors and acceptors without interference and to avoid the serious acceptor bleed-through resulting from the discrepancy between protein copy number and glycan abundance.[3b]

These problems can be solved by using a donor for single excitation to simultaneously and effectively activate multiple acceptors of large amount. Owing to the unique polychromatic light emitting properties, upconversion luminescent nanoparticles (UNPs) provide an excellent solution.[4] Multiple color emission from UNPs has been reported for nucleic acid assay and intracellular drug release monitoring.[4c,d] However, these systems were not designed for targeting a specific location, thus are not suitable for protein-specific glycoform study. This work used UNPs to construct a site-specific duplexed luminescence resonance energy transfer (D-LRET) system on cell surface for simultaneous imaging of different protein-specific monosaccharides using mucin 1 (MUC1) as the model protein (Scheme 1). The UNP exhibited two energy emission bands (EEB1 and EEB2) upon single excitation, each of which could only match to light up one kind of fluorescent dye in close proximity (within 10 nm)[5] through LRET, leading to a novel duplexed imaging strategy with single near-infrared excitation.

The target protein MUC1, known as CA15-3, is a tumor marker extensively O-glycosylated and overexpressed in a variety of epithelial cancers.[6] The extracellular section of MUC1 extends 200–500 nm beyond the cell surface and contains variable number of tandem repeat (VNTR) regions.[6a,b] Sialic acid (Sia) and fucose (Fuc) are the two common terminators of glycan chains which are suggested to be closely related to malignant transformation and oncogenesis,[1,7] thus were chosen as the sugars of interest. To achieve the designed duplexed imaging strategy, the monosaccharides and MUC1 were firstly labeled sequentially: metabolically labeling of monosaccharides on cell surface with different fluorescent dyes,[8] and specific recognition of MUC1 by aptamer-functionalized UNP (Apt-UNP) (Scheme 1 A). The targeting of the UNP to MUC1 was enabled by functionalization of UNP using aptamer S2.2, which is a 25-mer with high binding affinity toward individual repeat of VNTR on MUC1 and smaller volume than antibodies.[9] Thus multiple Apt-UNP could be assembled on each MUC1 polypeptide backbone. Upon a continuous-wave single excitation at 980 nm, two EEBs of UNP could be regarded as two

[*] N. Wu, L. Bao, Prof. Dr. L. Ding, Prof. Dr. H. Ju
State Key Laboratory of Analytical Chemistry for Life Science
School of Chemistry and Chemical Engineering
Nanjing University, Nanjing 210023 (P.R. China)
E-mail: dinglin@nju.edu.cn
hxju@nju.edu.cn

Supporting information for this article can be found under: http://dx.doi.org/10.1002/anie.201601233.

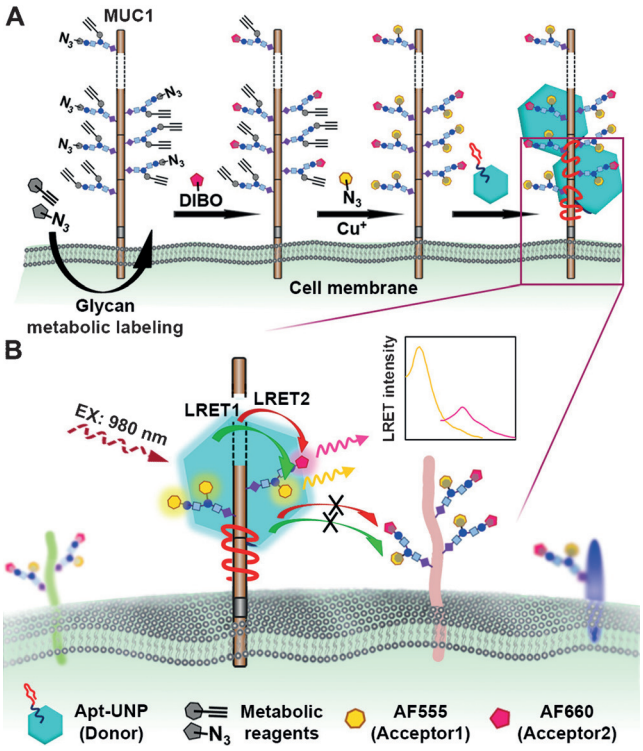

Scheme 1. The site-specific D-LRET method for duplexed imaging and dynamic monitoring of protein-specific monosaccharides on an intact cell surface. A) Two kinds of monosaccharides and the underlying protein were sequentially tagged with fluorescence acceptor dyes and aptamer-functionalized UNP (Apt-UNP) as a donor by dual metabolic labeling and aptamer recognition, respectively. B) Upon excitation at 980 nm, two non-interfering paralleled energy transfer processes from UNP to two acceptors displayed the existence of corresponding monosaccharides.

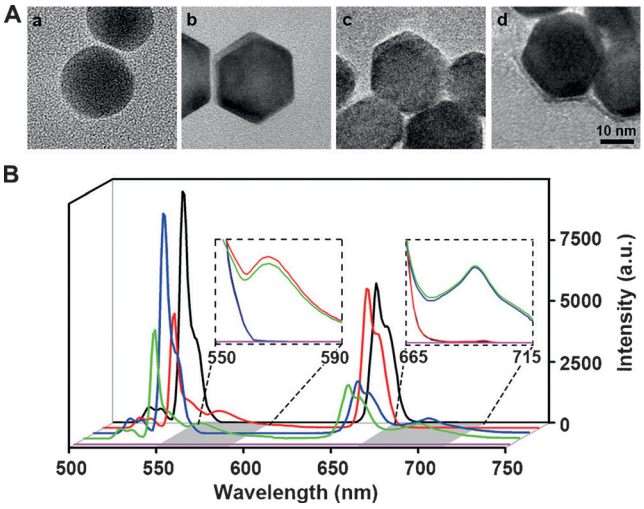

Figure 1. A) TEM images of core UNP (a), core–shell UNP (b), oleate-free UNP (c), and Apt-UNP (d). B) Emission spectra of A30-UNP (black), A30-UNP after hybridizing with AF555-T6 (red), AF660-T6 (blue), and both (green), and the mixture of AF555-T6 and AF660-T6 (magenta). Excitation wavelength: 980 nm.

independent energy donors. Only the fluorescence of acceptors clicked to MUC1-linked glycans could be lit up (Scheme 1 B). Distinct metabolically labeled glycoforms of MUC1 among different cell lines could be compared using the D-LRET strategy. In particular, through assigning *N*-acetylgalactosamine (GalNAc), the initial monosaccharide at *O*-glycosylated site,[6a,7] as the reference, this work proposed a quantitative strategy for obtaining the relative expression ratio of different metabolically labeled terminal sugars on MUC1, thus providing a strategy to dynamically monitor the terminal glycan pattern change in response to drugs. Compared with previous FRET systems,[3] this strategy featured two paralleled and non-interfering energy transfer processes by single near-infrared excitation. In particular, this work exploited an upconversion process to avoid acceptor spectral bleed-through, which is a major problem in current FRET-based protein-specific glycan imaging.[3b]

To construct the site-specific D-LRET system, a core–shell UNP, $NaYF_4$:Er/Gd/Yb(2/10/18%)@$NaGdF_4$ wrapped with oleate, was synthesized.[10a] Transmission electron microscopic (TEM) images suggested a hexagonal morphology of the core–shell UNP with a uniform diameter around 25 nm (Figure 1 A). The luminous efficiency of the core–shell UNP was about 6.5 fold that of core-only UNP (Supporting Information, Figure S1). After removing oleate with HCl, the UNP was linked to a T21-conjugated aptamer S2.2 (Apt) using a carboxylic group-modified oligonucleotide (A30-COOH) as the linker and particle stabilizer (Figure 1 A; Supporting Information, Figure S2A).[10b] The step-by-step assembly of the Apt-UNP was characterized in the Supporting Information, Figure S2B–G, and the amount of Apt conjugated to each UNP was estimated to be 3 (Supporting Information). The specific recognition of Apt (Figures S3 and S4) and Apt-UNP (Figures S5 and S6) toward MUC1 was verified using MCF-7 (MUC1-positive) and HepG2 (MUC1-negative) cells (Figure S7).[11] The scanning electron microscopic images and co-localization experiment also demonstrated the binding of Apt-UNP to MUC1 in a string-like arrangement on MCF-7 cells (Figure S6).

The luminescent intensity of the A30-COOH stabilized UNP (A30-UNP) and the feasibility of using A30-UNP to construct D-LRET system were evaluated in vitro. The upconversion luminescence (UCL) spectrum presented two sharp energy emission bands (EEB1: 530 to 560 nm, EEB2: 640 to 670 nm) with almost zero spectral baseline (Figure 1 B). Fluorescent dyes Alexa Fluor 555 (AF555) and Alexa Fluor 660 (AF660) were chosen as the acceptors to match the two emissions of UNP (Supporting Information, Figure S8). A30-UNP was subjected to hybridize with either AF555 or AF660 labeled oligonucleotide T6 (T6-AF555 or T6-AF660), or both. The orthogonality of the two LRET processes was demonstrated by the two LRET peaks at 570 (LRET1) and 690 nm (LRET2), respectively, with signal intensity almost invariant to those in single LRET system (Figure 1 B). Owing to the partial spectral overlap of two acceptors, the mutual influence between LRET1 and LRET2 was further examined, which showed negligible effect (Supporting Information, Figures S9 and S10). Notably, two T6-dyes did not exhibit observable signal under 980 nm excitation even at high concentration of 10 μM (Figure 1 B,

magenta), indicating a unique advantage of using UNP as the donor for avoiding acceptor spectral bleed-through. The signal intensity of LRET peaks exhibited a linear relationship with the acceptor concentration up to 1.2 μM (Supporting Information, Figure S11), enabling quantitative detection of protein-specific sugars on cell surface.

A single LRET system in site-specific format was then constructed on cell surface for imaging of MUC1-specific Fuc. The Fuc on MCF-7 cells was metabolically labeled and then clicked by AF555-azide. Under 980 nm excitation by confocal laser scanning microscopy (CLSM), an obvious AF555 fluorescence signal was observed around MCF-7 cells (Figure 2), which could be attributed to the LRET between

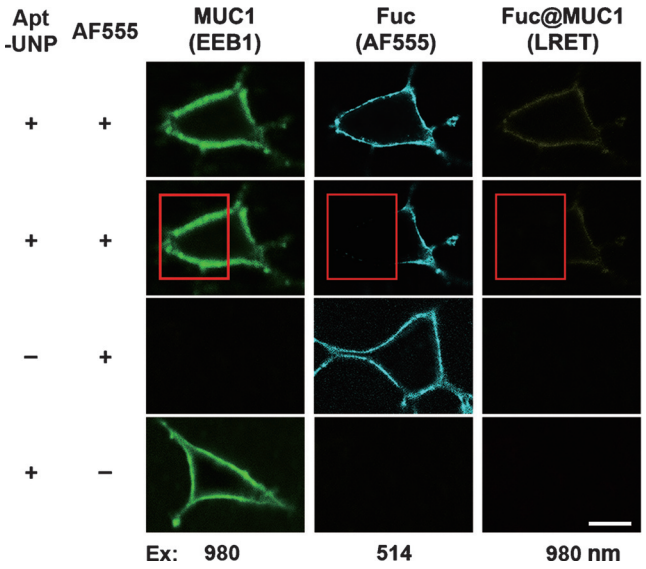

Figure 2. Protein-specific imaging of metabolically labeled Fuc on cell surface MUC1 by single LRET. Scale bar: 10 μm.

EEB1 of UNP and AF555. Since LRET could only generate when the donor–acceptor distance was less than 10 nm,[5] the obtained signal reflected the expression level of metabolically labeled Fuc only expressed on MUC1-specific glycan chains. To verify the energy transfer process, a series of control tests were performed. After photobleaching of acceptor AF555, the LRET signal disappeared along with dequenching of the UCL, and the cells labeled with AF555-azide or Apt-UNP alone showed only AF555 fluorescence (Ex: 514 nm) or UCL (Ex: 980 nm) with disappearance of LRET (Figure 2). The emission spectra on the cell surface collected by CLSM under 980 nm (Supporting Information, Figure S12) were consistent with the imaging data (Figure 2). Notably, in the absence of Apt-UNP, the AF555-labeled cells exhibited a straight line, indicating no bleed-through signal even when acceptor was in large excess. Also, this single LRET process did not influence the other EEB peak (Supporting Information, Figure S12), suggesting the possibility to construct D-LRET system on cell surface MUC1.

A site-specific D-LRET system was developed to implement duplexed imaging of two kinds of monosaccharides of MUC1 on cell surface using Sia and Fuc as the targets. Cell surface Fuc and Sia were metabolically labeled with AF555 and AF660 respectively (Supporting Information, Figure S13) using a dual metabolic labeling protocol,[8a] followed by tagging MUC1 with Apt-UNP. Under excitation at 980 nm, both AF555 and AF660 fluorescence could be observed in the cell membrane region (Figure 3; Supporting Information,

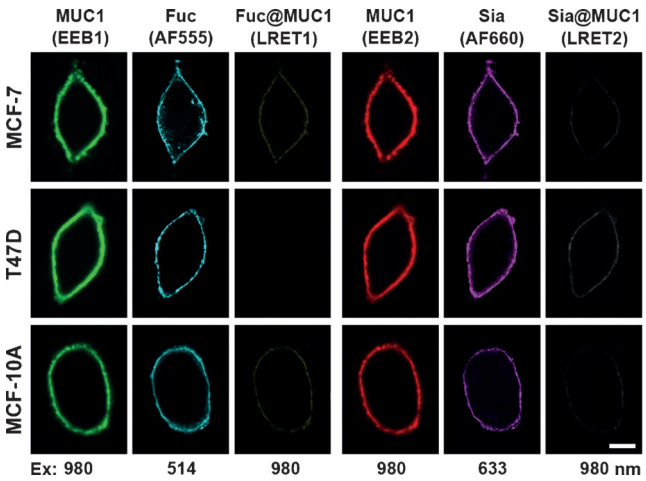

Figure 3. Duplexed protein-specific imaging of metabolically labeled Fuc and Sia of MUC1 on MCF-7, T47D and MCF-10A cells. Scale bar: 10 μm.

Figure S14), which could be attributed to the simultaneous LRET from the two EEBs of Apt-UNP to the two dyes (Supporting Information, Figure S15). The LRET signals suggested the existence of the corresponding metabolically labeled sugars on MUC1. The expression of Fuc and Sia of MUC1 on two types of tumor cells (MCF-7, T47D) and one type of normal cells (MCF-10A) were further studied. These cells are all of epithelial type from human mammary gland. MCF-7 and MCF-10A cells express both Fuc and Sia on MUC1, while T47D cells exhibit only MUC1-specific Sia. The absence of MUC1-specific Fuc on T47D cells is due to the loss of Core 2 β1-6-GlcNAc-transferase activity.[6a,b,7b] These results suggested the importance of using the proposed strategy to uncover protein-specific glycosylation information masked by global detection techniques. The observed distinct terminal patterns of metabolically labeled MUC1 glycoforms on three types of cells were in good agreement with literature reports,[6,7b,12a] thus could be used to differentiate different cell phenotypes.

Considering the obvious global Fuc signal on T47D and indiscernible LRET signal for Fuc on MUC1 (Figure 3), it could be deduced that the observed LRET luminescence was exactly from MUC1 rather than adjacent proteins. The protein-specific signal was further verified by tunicamycin inhibition experiment (Supporting Information, Figure S16).[3c] After blocking *N*-linked glycosylation with tunicamycin, the cell surface D-LRET signal was not affected by the absence of *N*-glycans. The unique structure of mucin family[6b,c] ensured the differentiation of protein-specific monosaccharaides even using a UNP with diameter of 25 nm as the donor.

To achieve relative quantification of two kinds of metabolically labeled terminal monosaccharaides (Fuc and Sia) of MUC1, GalNAc, the sugar initiates O-glycosylation at serine or threonine of MUC1 peptide chain,[6a,b,7] was chosen as the native reference, to exclude the influence due to the difference of the relative intensity and energy transfer efficiency between two donor dyes. Duplexed imaging of Fuc and GalNAc, as well as Sia and GalNAc of MUC1 on MCF-7 (Figure 4A), T47D (Supporting Information, Figure S17) and

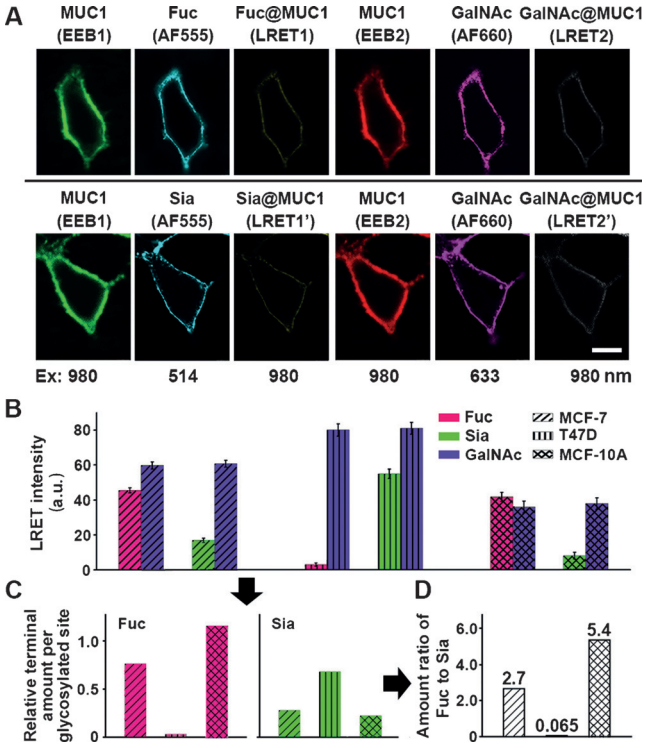

Figure 4. A) Duplexed protein-specific imaging of metabolically labeled Fuc and GalNAc (top), Sia and GalNAc (bottom) of MUC1 on MCF-7 cells, scale bar: 10 μm. B) LRET intensities for Fuc (LRET1) and GalNAc (LRET2), Sia (LRET1′) and GalNAc (LRET2′) of MUC1 on MCF-7, T47D and MCF-10A cells. C) Relative Fuc or Sia terminal amount per glycosylated site, and D) amount ratio of metabolically labeled Fuc to Sia of MUC1 on 3 cell types. Averages of the LRET intensity were measured on 10 individual cells for each experiment.

MCF-10A (Supporting Information, Figure S18) cells were, respectively performed by assigning GalNAc as the LRET2 reference, followed by acquiring LRET intensity of each channel (Figure 4B). Considering that the amount of GalNAc at MUC1 glycoforms is equivalent to the amount of O-glycosylated sites,[6a,b,7b,12a] the proportion of LRET1 to LRET2 could be regarded as the abundance of metabolically labeled Fuc (or Sia) terminal averaged over O-glycosylated site. Further, through acquiring the ratio of Sia terminal to Fuc terminal per O-glycosylated site, the ratio of metabolically labeled Fuc to Sia expressed on MUC1 glycoforms could be obtained as 2.7:1, 0.065:1 and 5.4:1 for MCF-7, T47D and MCF-10A cells, respectively (Figure 4D). The LRET intensity was also verified through analyzing LRET efficiency by CLSM for each pair of monosaccharides on MCF-7 cells (Supporting Information, Figure S19). The different ratios of metabolically labeled Fuc to Sia on MUC1 for different cell types might be partly caused by different levels of key glycosyltransferase activity governing the extension and termination of O-glycans,[6a,b,7b,12] and the difference of sugar analog labeling extent. The ratio of Fuc to Sia offered a desirable parameter for monitoring the dynamic change of terminal glycans on the target protein. During incubation with a model drug, neuraminidase, the change percentage of the ratio for MUC1 on MCF-7 cells increased remarkably due to the specific cleavage of Sia by neuraminidase (Supporting Information, Figure S20). This result demonstrated that the proposed method could be used to track protein-specific terminal glycan pattern.

In conclusion, this work provides a smart solution to implement duplexed imaging of protein-specific glycoforms on cell surface. The UNP oriented at MUC1 can be used as the single donor for two acceptors labeled on two monosaccharides, respectively, leading to two non-interfering LRET processes. The near-infrared excitation and upconversion process have been exploited to avoid acceptor spectral bleed-through, which is a unique advantage particularly significant when the glycans (acceptor) are in huge excess compared with the underlying protein (donor). The D-LRET system has been successfully employed for duplexed imaging and quantification of the ratio of metabolically labeled Fuc to Sia among different cell lines, as well as tracing of dynamic terminal pattern change on MUC1. The proposed single excitation-duplexed imaging strategy is compatible with other glycan labeling techniques and protein tagging methods. For smaller target proteins, this method can be employed by using UNPs with sub-10 nm diameter.[4b] With more click pairs available and other rare-earth elements for tuning UNP emission, it can be expanded to multi-channel imaging of protein-specific glycoforms. Thus this method could contribute to the understanding of the complex machinery of protein post-transcriptional modification, and provide a powerful platform for developing glycan-related biomarkers and glycan-targeted drugs.

Acknowledgements

We gratefully acknowledge National Basic Research Program (2014CB744501) and National Natural Science Foundation of China (21322506, 21135002, 91213301, 91413118).

Keywords: carbohydrates · duplexed LRET · nanoparticles · near-IR excitation · protein-specific imaging

How to cite: *Angew. Chem. Int. Ed.* **2016**, *55*, 5220–5224
Angew. Chem. **2016**, *128*, 5306–5310

[1] a) S. T. Laughlin, C. R. Bertozzi, *Proc. Natl. Acad. Sci. USA* **2009**, *106*, 12–17; b) D. H. Dube, C. R. Bertozzi, *Nat. Rev. Drug Discovery* **2005**, *4*, 477–488; c) D. P. Gamblin, E. M. Scanlan, B. G. Davis, *Chem. Rev.* **2009**, *109*, 131–163.
[2] a) P. Umaña, J. Jean-Mairet, R. Moudry, H. Amstutz, J. E. Bailey, *Nat. Biotechnol.* **1999**, *17*, 176–180; b) S. M. Chen, T. LaRoche, D. Hamelinck, D. Bergsma, D. Brenner, D. Simeone,

R. E. Brand, B. B. Haab, *Nat. Methods* **2007**, *4*, 437 – 444; c) K. O. Lloyd, J. Burchell, V. Kudryashov, B. W. T. Yin, J. Taylor-Papadimitriou, *J. Biol. Chem.* **1996**, *271*, 33325 – 33334.

[3] a) Y. Haga, K. Ishii, K. Hibino, Y. Sako, Y. Ito, N. Taniguchi, T. Suzuki, *Nat. Commun.* **2012**, *3*, 907; b) B. Belardi, A. de la Zerda, D. R. Spiciarich, S. L. Maund, D. M. Peehl, C. R. Bertozzi, *Angew. Chem. Int. Ed.* **2013**, *52*, 14045 – 14049; *Angew. Chem.* **2013**, *125*, 14295 – 14299; c) W. Lin, Y. F. Du, Y. T. Zhu, X. Chen, *J. Am. Chem. Soc.* **2014**, *136*, 679 – 687; d) F. Doll, A. Buntz, A. Spate, V. F. Schart, A. Timper, W. Schrimpf, C. R. Hauck, A. Zumbusch, V. Wittmann, *Angew. Chem. Int. Ed.* **2016**, *55*, 2262 – 2266; *Angew. Chem.* **2016**, *128*, 2303 – 2308; e) W. Lin, L. Gao, X. Chen, *ChemBioChem* **2015**, *16*, 2571 – 2575.

[4] a) Q. Q. Su, S. Y. Han, X. J. Xie, H. M. Zhu, H. Y. Chen, C. K. Chen, R. S. Liu, X. Y. Chen, F. Wang, X. G. Liu, *J. Am. Chem. Soc.* **2012**, *134*, 20849 – 20857; b) G. Y. Chen, H. L. Qiu, P. N. Prasad, X. Chen, *Chem. Rev.* **2014**, *114*, 5161 – 5214; c) F. Zhou, U. J. Krull, *Anal. Chem.* **2014**, *86*, 10932 – 10939; d) J. P. Lai, B. P. Shah, Y. X. Zhang, L. T. Yang, K.-B. Lee, *ACS Nano* **2015**, *9*, 5242 – 5245.

[5] H. C. Guo, N. M. Idris, Y. Zhang, *Langmuir* **2011**, *27*, 2854 – 2860.

[6] a) S. Nath, P. Mukherjee, *Trends Mol. Med.* **2014**, *20*, 332 – 342; b) F. G. Hanisch, S. Müller, *Glycobiology* **2000**, *10*, 439 – 449; c) M. A. Hollingsworth, B. J. Swanson, *Nat. Rev. Cancer* **2004**, *4*, 45 – 60.

[7] a) X. L. Song, R. D. Airan, D. R. Arifin, A. Bar-Shir, D. K. Kadayakkara, G. S. Liu, A. A. Gilad, P. C. M. van Zijl, M. T. McMahon, J. W. M. Bulte, *Nat. Commun.* **2015**, *6*, 6719; b) I. Brockhausen, J. M. Yang, J. Burchell, C. Whitehouse, J. Taylor-Papadimitriou, *Eur. J. Biochem.* **1995**, *233*, 607 – 617.

[8] a) L. S. Feng, S. L. Hong, J. Rong, Q. C. You, P. Dai, R. B. Huang, Y. H. Tan, W. Y. Hong, C. Xie, J. Zhao, X. Chen, *J. Am. Chem. Soc.* **2013**, *135*, 9244 – 9247; b) P. V. Chang, X. Chen, C. Smyrniotis, A. Xenakis, T. S. Hu, C. R. Bertozzi, P. Wu, *Angew. Chem. Int. Ed.* **2009**, *48*, 4030 – 4033; *Angew. Chem.* **2009**, *121*, 4090 – 4093.

[9] A. B. Iliuk, L. H. Hu, W. A. Tao, *Anal. Chem.* **2011**, *83*, 4440 – 4452.

[10] a) J. N. Liu, W. B. Bu, L. M. Pan, J. L. Shi, *Angew. Chem. Int. Ed.* **2013**, *52*, 4375 – 4379; *Angew. Chem.* **2013**, *125*, 4471 – 4475; b) L. L. Li, P. W. Wu, K. Hwang, Y. Lu, *J. Am. Chem. Soc.* **2013**, *135*, 2411 – 2414.

[11] M. V. Croce, M. T. Isla-Larrain, A. Capafons, M. R. Price, A. Segal-Eiras, *Breast Cancer Res. Treat.* **2001**, *69*, 1 – 11.

[12] a) S. Muller, F. G. Hanisch, *J. Biol. Chem.* **2002**, *277*, 26103 – 26112; b) Z. X. Lin, D. M. Simeone, M. A. Anderson, R. E. Brand, X. L. Xie, K. A. Shedden, M. T. Ruffin, D. M. Lubman, *J. Proteome Res.* **2011**, *10*, 2602 – 2611; c) C. J. Bosques, S. Raguram, *R. Sasisekharan, Nat. Biotechnol.* **2006**, *24*, 1100 – 1101.

Received: February 3, 2016
Published online: March 22, 2016

